Pattern selection in steady binary-fluid convection

Mary Silber and Edgar Knobloch
Department of Physics, University of California, Berkeley, California 94720
(Received 11 February 1988)

Three-dimensional convection in a binary-fluid mixture is studied near the onset of the steady-state instability using symmetric bifurcation theory. Idealized boundary conditions are assumed in which the temperature and solute concentration are fixed at top and bottom, with stress-free boundary conditions on the velocity field. The effects of sidewalls are neglected. The problem is formulated as a bifurcation problem on a doubly periodic lattice, with two cases considered in detail: the square lattice and the hexagonal lattice. Symmetry considerations determine the form of the ordinary differential equations governing the dynamics of the neutrally stable modes. The relevant coefficients of these equations are calculated from the governing binary-fluid equations. The bifurcation diagrams are given for all physical values of the separation ratio, the Lewis number, and the Prandtl number. It is found that supercritical rolls are stable to all perturbations lying on the square and hexagonal lattices. Squares, hexagons, and triangles are never stable for the physically accessible regions of parameter space.

I. INTRODUCTION

Rayleigh-Bénard convection has been extensively studied as a relatively simple pattern forming system. These studies have emphasized those solutions that are spatially periodic along with their stability properties. Disordered patterns have begun to be studied only relatively recently. The emphasis on spatially periodic patterns stems from the prevalence of approximately periodic patterns in carefully controlled experiments. The observed patterns depend on the specifics of the system. Thus rolls are stable in systems with a reflection symmetry in the layer midplane,[1] while stable hexagons appear in a hysteretic bifurcation in systems in which small non-Boussinesq effects are important.[2] Stable squares are found in convection with a strongly temperature-dependent viscosity[3] or in Boussinesq convection between thermally insulating plates.[4]

The initial bifurcation leading to the above patterns is a steady-state one. Recent years have seen increasing interest in pattern formation arising from a Hopf bifurcation, and this has lead investigators to study convection in binary fluid mixtures. These experiments have resulted in the discovery of a number of novel phenomena, the most interesting being the variety of travelling patterns that are possible.[5] In addition, stationary patterns in three dimensions have also been investigated. Of particular interest here is the transition between squares and rolls observed by Moses and Steinberg,[6] and Le Gal, Pocheau, and Croquette.[7] Hexagons, though possible in systems with midplane reflection symmetry, have not been found.

The present paper is a first step towards an understanding of the relative stability of various three-dimensional time-independent patterns in binary fluid mixtures. We consider an unbounded Boussinesq fluid confined between two parallel highly conducting plates, the lower of which is maintained at a higher temperature than the upper. The resulting equations are then equivariant under the group $\Gamma = E(2) \times \mathbb{Z}_2$, where E(2) is the Euclidean group that preserves the horizontal plane, and $\mathbb{Z}_2$ is a reflection in the midplane of the layer. In order to apply the results of bifurcation theory, we seek solutions that are doubly periodic in the plane and lie either on the square or hexagonal lattices. This formulation introduces the compact groups $\Gamma_S \equiv D_4 \times T^2 \times \mathbb{Z}_2$ or $\Gamma_H \equiv D_6 \times T^2 \times \mathbb{Z}_2$ and renders the number of critical eigenvalues finite. The mathematical techniques used to study such problems are those of equivariant bifurcation theory and singularity theory,[8] and enable us to rigorously establish the relative stability between rolls and squares on the square lattice, and between rolls, hexagons, regular triangles, and rectangles on the hexagonal lattice. These techniques have already been used to classify the secondary bifurcations that occur on the hexagonal lattice without reflection symmetry[9,10] and thereby to complete the analysis begun by Busse.[2]

In Sec. II we introduce the basic equations and the boundary conditions, and indicate the resulting symmetries. The results of linear stability theory are also briefly summarized. In Sec. III the mathematical results concerning the form of the amplitude equations on the two lattices are given. This analysis provides an abstract classification of the possible behavior and depends only on the symmetries. It indicates exactly what perturbation calculations need to be done in order that specific predictions about a given physical system can be made. These calculations are performed in Sec. IV and the results discussed in Sec. V. With the boundary conditions considered we find that in both cases the only possible stable pattern near onset is *rolls*. This supports the suggestion[6] that the zero mass flux boundary condition is essential in stabilizing squares.[4]

II. FORMULATION OF THE PROBLEM

A. Basic equations

The nondimensionalized Boussinesq equations describing convection in a binary fluid take the form[11,12]

$$\left[\frac{\partial}{\partial t}-\sigma\nabla^2\right]\mathbf{u}-R\sigma(\theta+S\Sigma)\hat{\mathbf{y}}+\nabla p=-\mathbf{u}\cdot\nabla\mathbf{u}\ , \tag{2.1a}$$

$$\left[\frac{\partial}{\partial t}-\nabla^2\right]\theta-w=-\mathbf{u}\cdot\nabla\theta\ , \tag{2.1b}$$

$$\left[\frac{\partial}{\partial t}-\tau\nabla^2\right]\Sigma+\tau\nabla^2\theta-w=-\mathbf{u}\cdot\nabla\Sigma\ , \tag{2.1c}$$

$$\nabla\cdot\mathbf{u}=0\ . \tag{2.1d}$$

Here $\mathbf{u}\equiv(u,v,w)$ is the velocity field in (x_1,x_2,y) coordinates, θ and Σ denote nondimensional departures of the temperature and concentration from their conduction profiles, and p is the pressure perturbation. The equations depend on four dimensionless parameters, the Prandtl and Lewis numbers σ and τ, the Rayleigh number R, and the separation ratio S. The separation ratio S is proportional to the Soret coefficient. When S is positive the heavier solute migrates towards the colder (upper plate), adding to the destabilizing effect of the imposed temperature difference. When S is negative the solute distribution set up by the Soret effect opposes the destabilizing effect of the temperature difference; consequently, when S is sufficiently negative the initial instability can occur via a Hopf bifurcation. The Dufour effect has been neglected.

B. Boundary conditions

Equations (2.1) are supplemented with stress-free boundary conditions and fixed temperature and concentration at the top and bottom plates:

$$w=\theta=\Sigma=\frac{\partial u}{\partial y}=\frac{\partial v}{\partial y}=0\quad\text{on } y=0,1\ . \tag{2.2}$$

Although these boundary conditions are not appropriate to the experiments carried out thus far, they have the advantage that analytical calculations can be performed. In addition they allow us to compare our results with other problems where similar boundary conditions have been used.

C. Symmetries

With the boundary conditions (2.2) the equations of motion (2.1) are equivariant under the group E(2) of translations and rotations of the plane. For example, translations act by

$$\begin{aligned}&(x_1,x_2)\to(x_1+\lambda_1,x_2+\lambda_2)\ ,\\&(u,v,w,p,\theta,\Sigma)\to(u,v,w,p,\theta,\Sigma)\ .\end{aligned} \tag{2.3a}$$

In addition, the equations are equivariant with respect to reflection in the midplane, i.e., under the operation

$$y\to1-y,\quad(u,v,w,p,\theta,\Sigma)\to(u,v,-w,p,-\theta,-\Sigma)\ . \tag{2.3b}$$

Consequently the symmetry group of the problem is the group $\mathrm{E}(2)\times\mathbb{Z}_2$.

D. Linear stability properties

Equations (2.1) and (2.2) admit the conduction solution $(\mathbf{u},p,\theta,\Sigma)=(\mathbf{0},0,0,0)$. As the Rayleigh number is increased this solution loses stability at either a steady-state bifurcation (R^{SS}) or a Hopf bifurcation (R^{Hopf}); both critical Rayleigh numbers are minimized by the *same* wave number $k_c=\pi/\sqrt{2}$, and are then given by[11,12]

$$R^{\mathrm{SS}}=\frac{27\pi^4}{4}\frac{\tau}{\tau+S(\tau+1)}\ , \tag{2.4}$$

$$R^{\mathrm{Hopf}}=\frac{27\pi^4}{4}\frac{(\sigma+\tau)(1+\sigma)(1+\tau)}{\sigma[1+\sigma(S+1)]}\ . \tag{2.5}$$

The steady-state bifurcation sets in first provided

$$S>\frac{-\tau^2(\sigma+1)}{\sigma+\tau(\sigma+1)(\tau+1)}\ . \tag{2.6}$$

Note that with other boundary conditions the two critical Rayleigh numbers will be minimized by different wave numbers.[13,14] In particular, this is the case for no-slip boundary conditions that are appropriate to the recent experiments.[14] Indeed, for these boundary conditions and large enough positive S the critical wave number for the steady-state bifurcation vanishes, and the first instability has infinite wavelength.[14]

III. STEADY-STATE BIFURCATIONS ON SQUARE AND HEXAGONAL LATTICES

As posed there are two obstructions to the application of rigorous results from bifurcation theory. The first arises from the fact that the Euclidean group is noncompact. Consequently, the kernel of the linear operator describing the stability properties of the conduction state is infinite dimensional. In particular, the linear theory, while predicting the wave number k_c of the marginal modes, leaves their orientation unspecified, i.e., there is a whole circle of marginally stable modes. The second difficulty arises from the fact that the marginally stable eigenvalues at R^{SS} are not isolated: stable eigenvalues accumulate at zero. Consequently, for $R>R^{\mathrm{SS}}$ a whole band of unstable wave numbers appears. Both problems are overcome when we restrict attention to spatially periodic solutions in the plane of the form

$$\mathbf{f}(\mathbf{x},y)=\mathbf{f}(\mathbf{x}+n_1\mathbf{a}_1+n_2\mathbf{a}_2,y),\quad\mathbf{x}\equiv(x_1,x_2)\ , \tag{3.1}$$

where $\mathbf{a}_1,\mathbf{a}_2$ are generators of the lattice and n_1,n_2 are integers. This assumption reduces the symmetry of the problem (2.1) and (2.2) to the subgroup $\hat{\Gamma}\times T^2\times\mathbb{Z}_2$ of $\mathrm{E}(2)\times\mathbb{Z}_2$, where $\hat{\Gamma}$ is the symmetry of a unit cell, and the two torus describes the action of translations on doubly periodic functions of the form (3.1). The solutions can be written in the form

$$\mathbf{f}(\mathbf{x},y)=\mathrm{Re}\sum_{n_1,n_2}z_{n_1,n_2}e^{i(n_1\mathbf{k}_1+n_2\mathbf{k}_2)\cdot\mathbf{x}}\mathbf{f}_{n_1,n_2}(y)\ , \tag{3.2}$$

where $\mathbf{k}_1,\mathbf{k}_2$ are wave vectors on the reciprocal lattice: $\mathbf{k}_i\cdot\mathbf{a}_j=2\pi\delta_{ij}$. The complex amplitudes z_{n_1,n_2} specify the pattern. We choose $|\mathbf{k}_i|=k_c$. There are three possible lattices: square, hexagonal, and rhombic. In this paper

we consider the first two, for which the group $\hat{\Gamma}$ is D_4 and D_6, respectively. Thus the symmetry groups for the problem (2.1) and (2.2) on square and hexagonal lattices are

$$\Gamma_S = D_4 \times T^2 \times \mathbb{Z}_2, \quad \Gamma_H = D_6 \times T^2 \times \mathbb{Z}_2 . \tag{3.3}$$

A. Square lattice

The fundamental wave vectors of the square lattice may be chosen to be

$$\mathbf{k}_1 = k_c \hat{\mathbf{x}}_1, \quad \mathbf{k}_2 = k_c \hat{\mathbf{x}}_2 , \tag{3.4}$$

where $\hat{\mathbf{x}}_1, \hat{\mathbf{x}}_2$ denote orthonormal vectors in the horizontal plane. Then the kernel of the linearized problem at $R = R^{SS}$ is

$$w^S = \{(z_1 e^{ik_c x_1} + z_2 e^{ik_c x_2} + \text{c.c.}) \sin(\pi y) \mid (z_1, z_2) \in \mathbb{C}^2\} , \tag{3.5}$$

where w is the vertical velocity and c.c. denotes the complex conjugate. The center manifold theorem[15] justifies a description of the dynamics near $\mathbf{z} = (z_1, z_2) = \mathbf{0}, R = R^{SS}$ in terms of ordinary differential equations for the complex amplitudes,

$$\dot{\mathbf{z}} = \mathbf{g}(\mathbf{z}, \lambda), \quad g: \ \mathbb{C}^2 \times \mathbb{R} \to \mathbb{C}^2 , \tag{3.6}$$

where $\lambda = R - R^{SS}$. The form of these equations is determined by the symmetry Γ_S.

A translation in the horizontal (x_1, x_2) plane induces the following action on the amplitudes:

$$(s,t) \cdot (z_1, z_2) \mapsto (e^{is} z_1, e^{it} z_2), \quad (s,t) \in T^2 . \tag{3.7a}$$

The group D_4 is generated by a 90° rotation $r_{90°}$, and by a reflection σ_v which takes $x_2 \to -x_2$. The corresponding action on $\mathbb{C}^2$ is

$$r_{90°} \cdot (z_1, z_2) \mapsto (z_2, \bar{z}_1) , \tag{3.7b}$$

$$\sigma_v \cdot (z_1, z_2) \mapsto (z_1, \bar{z}_2) . \tag{3.7c}$$

The $\mathbb{Z}_2$-midplane reflection which takes $w(\mathbf{x}, y) \to -w(\mathbf{x}, 1-y)$ acts on $\mathbb{C}^2$ by $-I$. This action is equivalent to a translation $(\pi, \pi) \in T^2$, so that $D_4 \times T^2 \times \mathbb{Z}_2 \approx D_4 \times T^2$. In terms of real variables defined by $z_j = r_j e^{i\phi_j}, j = 1,2$, the most general $(D_4 \times T^2)$-equivariant vector field on $\mathbb{R}^4$ is[16]

$$\begin{pmatrix} \dot{r}_1 \\ \dot{r}_2 \end{pmatrix} = p \begin{pmatrix} r_1 \\ r_2 \end{pmatrix} + q\delta \begin{pmatrix} r_1 \\ -r_2 \end{pmatrix} , \tag{3.8}$$

$$\dot{\phi}_1 = \dot{\phi}_2 = 0 ,$$

where p and q are smooth real-valued functions of $N \equiv r_1^2 + r_2^2$, $\Delta = \delta^2 \equiv (r_2^2 - r_1^2)^2$, and λ. Observe that the equations for the amplitudes (r_1, r_2) have decoupled from the phase equations and that they have D_4 symmetry.[17]

The singularity theory normal form of the steady-state bifurcation problem is of finite order and is given by[16]

$$\mathbf{n}(r_1, r_2, \lambda) = (\varepsilon_0 \lambda + mN) \begin{pmatrix} r_1 \\ r_2 \end{pmatrix} + \varepsilon_1 \delta \begin{pmatrix} r_1 \\ -r_2 \end{pmatrix} , \quad m \neq 0, \varepsilon_1 , \tag{3.9}$$

provided that the following nondegeneracy conditions hold for (3.8):

$$p_\lambda \neq 0, \quad p_N \neq 0, \quad q \neq 0, \quad p_N \neq q \quad \text{at } N = \Delta = \lambda = 0 , \tag{3.10}$$

where the subscripts denote partial derivatives. The zeros of $\mathbf{n}$ are in one-to-one correspondence with those of (3.8). The coefficients $m, \varepsilon_0, \varepsilon_1$ are related to coefficients in the Taylor expansion of (3.8) about $r_1 = r_2 = \lambda = 0$,

$$\varepsilon_0 = \text{sgn}(p_\lambda), \quad \varepsilon_1 = \text{sgn}(q), \quad m = \frac{p_N}{|q|} . \tag{3.11}$$

From the linear problem we know that the trivial solution is stable subcritically, and therefore that $\varepsilon_0 = +1$.

There are two types of nontrivial solutions to (3.9) corresponding to rolls (R), and squares (S):
(R),

$$r_1 \neq 0, \quad r_2 = 0 , \tag{3.12a}$$

(S),

$$r_1 = r_2 \neq 0 . \tag{3.12b}$$

These solutions may be determined in terms of the coordinates of the original equivariant vector field (3.8) by restricting its Taylor expansion to the invariant subspaces (3.12). Thus for (R),

$$r_1^2 = \frac{p_\lambda \lambda}{(q - p_N)} + \mathcal{O}(\lambda^2), \quad r_2 = 0 , \tag{3.13a}$$

and for (S),

$$r_1^2 = r_2^2 = -\frac{p_\lambda \lambda}{2p_N} + \mathcal{O}(\lambda^2) . \tag{3.13b}$$

In Fig. 1 the bifurcation diagrams associated with the normal form (3.9) are shown in the various regions of the (m, ε_1) space. Note that both branches must be supercritical in order that there be a stable nontrivial solution. Which of the two branches is actually stable depends on the value of ε_1. The values of the coefficients m, ε_1 as

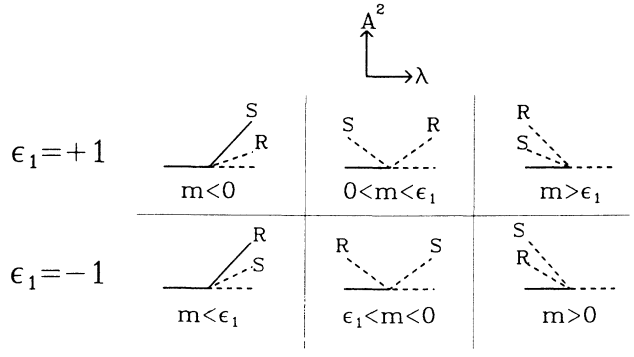

FIG. 1. Bifurcation diagrams for $\varepsilon_0 = +1$ and all values of the coefficients ε_1 and m in the general D_4-equivariant normal form (3.9) showing the variation in amplitude with the bifurcation parameter λ for rolls (R) and squares (S). The trivial solution, corresponding to $r_1 = r_2 = 0$, is indicated by a horizontal line in the diagrams. Stable solutions are denoted by a solid line and unstable solutions by a dashed line.

functions of the physical parameters (S,τ,σ) may be calculated from the partial differential equations (2.1) and (2.2) by considering steady-state solutions in the form of rolls and squares. Let A_R and A_S denote the amplitudes of the rolls and squares. Then for small A_R and A_S we may expand the Rayleigh number about its critical value $R=R^{SS}+A_R^2R_2^R+\cdots$, and likewise for squares. Thus for (R),

$$A_R^2=\frac{\lambda}{R_2^R}+\cdots , \tag{3.14a}$$

and for (S),

$$A_S^2=\frac{\lambda}{R_2^S}+\cdots . \tag{3.14b}$$

Direct comparison of (3.14) with (3.13) together with Eqs. (3.11) now determines ε_1 and m in terms of R_2^R and R_2^S,

$$\begin{aligned}\varepsilon_1&=\mathrm{sgn}(2R_2^R-R_2^S) ,\\ m&=\left|\frac{\varepsilon_1 R_2^S}{R_2^S-2R_2^R}\right| .\end{aligned} \tag{3.15}$$

The quantities R_2^R and R_2^S are calculated in Sec. IV.

B. Hexagonal lattice

In this case the center manifold is spanned by three complex amplitudes with the kernel of the linearized equations at $R=R^{SS}$ given by

$$\begin{aligned}w^H=\{&(z_1e^{ik_cx_1}+z_2e^{ik_c(\sqrt{3}x_2-x_1)/2}\\&+z_3e^{-ik_c(\sqrt{3}x_2+x_1)/2}\\&+\mathrm{c.c.})\sin(\pi y)\mid(z_1,z_2,z_3)\in\mathbb{C}^3\} .\end{aligned} \tag{3.16}$$

The action of $D_6\times T^2$ on $\mathbb{C}^3$ may be determined in a similar fashion to that described for the square lattice. However, in this case the $\mathbb{Z}_2$-midplane reflection is not equivalent to a translation so that the appropriate symmetry group is $D_6\times T^2\times\mathbb{Z}_2$. The general $(D_6\times T^2\times\mathbb{Z}_2)$ equivariant vector field is[10]

$$\begin{aligned}\dot{z}_1&=z_1(l_1+u_1l_3+u_1^2l_5)+\bar{z}_2\bar{z}_3q(m_5+u_1m_7+u_1^2m_9) ,\\ u_1&\equiv|z_1^2| ,\end{aligned} \tag{3.17}$$

with the corresponding equations for z_2 and z_3 obtained by cyclic permutation. The quantities l_j, and m_j are functions of λ and the invariants,

$$\begin{aligned}\sigma_1&\equiv u_1+u_2+u_3 ,\\ \sigma_2&\equiv u_1u_2+u_2u_3+u_3u_1 ,\\ \sigma_3&\equiv u_1u_2u_3 ,\\ q^2&\equiv(z_1z_2z_3+\bar{z}_1\bar{z}_2\bar{z}_3)^2 .\end{aligned} \tag{3.18}$$

There are four nontrivial solutions to $\dot{\mathbf{z}}=\mathbf{g}(\mathbf{z},\lambda)=\mathbf{0}$, $\mathbf{z}=(z_1,z_2,z_3)$, on a neighborhood of the bifurcation point $(\mathbf{z},\lambda)=\mathbf{0}$, provided the following nondegeneracy conditions hold:

$$\begin{aligned}&l_{1,\lambda}(\mathbf{0})\neq0,\quad l_{1,\sigma_1}(\mathbf{0})+l_3(\mathbf{0})\neq0 ,\\ &2l_{1,\sigma_1}(\mathbf{0})+l_3(\mathbf{0})\neq0,\quad 3l_{1,\sigma_1}(\mathbf{0})+l_3(\mathbf{0})\neq0 ,\\ &l_3(\mathbf{0})\neq0,\quad m_5(\mathbf{0})\neq0 .\end{aligned} \tag{3.19}$$

These four solutions correspond to rolls (R), hexagons, (H), regular triangles (RT), and a rectangular pattern called the patchwork quilt (PQ):

(R),

$$z_1\neq0,\quad z_2=z_3=0,\quad z_1\in\mathbb{R} , \tag{3.20a}$$

(H),

$$z_1=z_2=z_3\neq0,\quad z_1\in\mathbb{R} , \tag{3.20b}$$

(RT),

$$z_1=z_2=z_3\neq0,\quad iz_1\in\mathbb{R} , \tag{3.20c}$$

(PQ),

$$z_1=0,\quad z_2=z_3\neq0,\quad z_2\in\mathbb{R} . \tag{3.20d}$$

Upon rescaling time, the bifurcation parameter, and the amplitudes, the vector field takes the form

$$\dot{z}_1=z_1(\lambda+a\sigma_1+u_1)+cq\bar{z}_2\bar{z}_3+O(z^5,\lambda^2z,\lambda z^3) , \tag{3.21}$$

$$a\neq-1,\quad a\neq-\tfrac{1}{2},\quad a\neq-\tfrac{1}{3},\quad c=\pm1 ,$$

where

$$a=\frac{l_{1,\sigma_1}(\mathbf{0})}{l_3(\mathbf{0})},\quad c=\mathrm{sgn}[m_5(\mathbf{0})l_3(\mathbf{0})] . \tag{3.22}$$

The transformation which puts the amplitude equations in this form reverses the direction of time and changes the sign of λ if $l_3(\mathbf{0})<0$. The bifurcation diagrams are given in Fig. 2 for various values of a and $c=+1$ [for $c=-1$, the (H) and (RT) branches are interchanged]. Note that a stable solution exists only when all solution

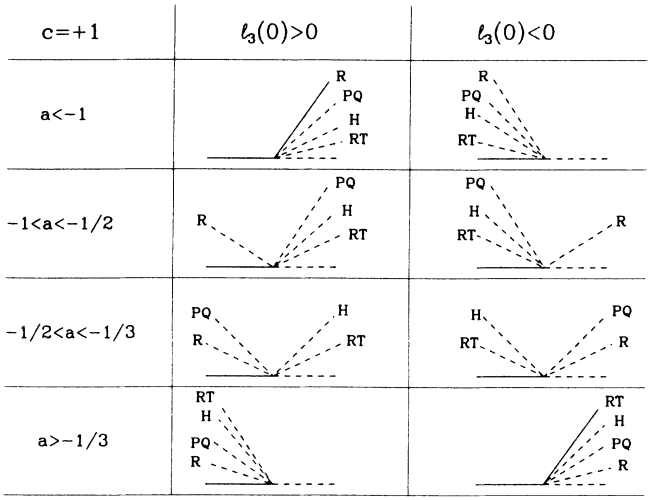

FIG. 2. Bifurcation diagrams for $c=+1$ and all values of the coefficient a in the general Γ_H- equivariant vector field (3.21). The diagrams for $c=-1$ are obtained by interchanging the (H) and (RT) branches.

branches bifurcate supercritically, and that the solution (PQ) is never stable on a neighborhood of the initial bifurcation.

The coefficient a and the sign of $l_3(\mathbf{0})$ may be computed from a third-order perturbation calculation of rolls and hexagons. As before, we let A_R and A_H denote the amplitudes of rolls and hexagons. Then for (R),

$$A_R^2=\frac{\lambda}{R_2^R}+\cdots\ , \tag{3.23a}$$

and for (H),

$$A_H^2=\frac{\lambda}{R_2^H}+\cdots\ . \tag{3.23b}$$

These solutions may be compared with the corresponding solutions of the equivariant vector field (3.17) restricted to the invariant subspaces of rolls and hexagons:

(R),

$$z_1^2=-\frac{l_{1,\lambda}\lambda}{(l_{1,\sigma_1}+l_3)}+O(\lambda^2),\quad z_2=z_3=0\ , \tag{3.24a}$$

(H),

$$z_1^2=z_2^2=z_3^2=-\frac{l_{l,\lambda}\lambda}{(3l_{1,\sigma_1}+l_3)}+O(\lambda^2)\ . \tag{3.24b}$$

The trivial solution is stable subcritically so that $\mathrm{sgn}(l_{1,\lambda})=+1$. On comparing (3.23) and (3.24) together with Eq. (3.22) we obtain

$$\begin{aligned} a&=\frac{R_2^R-R_2^H}{R_2^H-3R_2^R}\ ,\\ \mathrm{sgn}(l_3(\mathbf{0}))&=\mathrm{sgn}(R_2^H-3R_2^R)\ . \end{aligned} \tag{3.25}$$

The quantity R_2^H is calculated in Sec. IV.

The computation of the coefficient c requires fifth-order perturbative calculations of the hexagons and regular triangles. Such a calculation is necessary in order to distinguish between these two branches in the bifurcation diagrams. Since we find that neither of these solutions is ever stable for the physically accessible regions of parameter space, no fifth-order calculations have been done.

IV. CALCULATIONS AND RESULTS

In order to determine the coefficients m and ε_1 in the normal form (3.9) and the coefficient a in the vector field (3.21), we consider the steady-state form of Eqs. (2.1) and look for solutions in the form of rolls, squares, and hexagons. In doing these calculations it is convenient to decouple the linear part of the equation for the vertical velocity field w from the other fields. This is accomplished by taking the curl of Eq. (2.1a) twice, thereby eliminating the pressure p and the linear terms involving u and v from the $\hat{\mathbf{y}}$ component. Finally, linear terms in θ and Σ are eliminated by operating with $\tau\nabla^2$ on the resulting equation. The following steady-state equation for w is obtained:

$$L_0 w=\lambda L_1 w+N_1(\mathbf{u},\mathbf{u})+R[N_2(\mathbf{u},\theta)+N_3(\mathbf{u},\Sigma)]\ , \tag{4.1}$$

where

$$\lambda=R-R^{SS}\ . \tag{4.2}$$

Here L_0 and L_1 are the linear operators

$$\begin{aligned} L_0&=\tau\nabla^6-R^{SS}[\tau+S(1+\tau)]\nabla_h^2\ ,\\ L_1&=[\tau+S(1+\tau)]\nabla_h^2\ , \end{aligned} \tag{4.3}$$

where

$$\nabla_h^2=\frac{\partial^2}{\partial x_1^2}+\frac{\partial^2}{\partial x_2^2}\ . \tag{4.4}$$

$N_1(\mathbf{u},\mathbf{u})$, $N_2(\mathbf{u},\theta)$, and $N_3(\mathbf{u},\Sigma)$ represent the nonlinear terms

$$\begin{aligned} N_1(\mathbf{u},\mathbf{u})&=\frac{\tau}{\sigma}\nabla^2\left[\nabla_h^2(\mathbf{u}\cdot\nabla w)-\frac{\partial^2}{\partial x_1\partial y}(\mathbf{u}\cdot\nabla u)\right.\\ &\qquad\left.-\frac{\partial^2}{\partial x_2\partial y}(\mathbf{u}\cdot\nabla v)\right]\ ,\\ N_2(\mathbf{u},\theta)&=-\tau(1+S)\nabla_h^2(\mathbf{u}\cdot\nabla\theta)\ ,\\ N_3(\mathbf{u},\Sigma)&=-S\nabla_h^2(\mathbf{u}\cdot\nabla\Sigma)\ . \end{aligned} \tag{4.5}$$

The steady-state equations for u, v, θ, and Σ are

$$\begin{aligned} \nabla^4 u-R\frac{\partial^2}{\partial y\,\partial x_1}(\theta+S\Sigma)&=\frac{1}{\sigma}\left[\left(\frac{\partial^2}{\partial y^2}+\frac{\partial^2}{\partial x_2^2}\right)(\mathbf{u}\cdot\nabla u)\right.\\ &\qquad-\frac{\partial^2}{\partial x_1\partial x_2}(\mathbf{u}\cdot\nabla v)\\ &\qquad\left.-\frac{\partial^2}{\partial x_1\partial y}(\mathbf{u}\cdot\nabla w)\right]\ ,\\ \nabla^4 v-R\frac{\partial^2}{\partial y\,\partial x_2}(\theta+S\Sigma)&=\frac{1}{\sigma}\left[\left(\frac{\partial^2}{\partial y^2}+\frac{\partial^2}{\partial x_1^2}\right)(\mathbf{u}\cdot\nabla v)\right.\\ &\qquad-\frac{\partial^2}{\partial x_1\partial x_2}(\mathbf{u}\cdot\nabla u)\\ &\qquad\left.-\frac{\partial^2}{\partial x_2\partial y}(\mathbf{u}\cdot\nabla w)\right]\ , \end{aligned} \tag{4.6}$$

$$\nabla^2\theta+w=\mathbf{u}\cdot\nabla\theta,\quad \tau(\nabla^2\Sigma-\nabla^2\theta)+w=\mathbf{u}\cdot\nabla\Sigma,\quad \nabla\cdot\mathbf{u}=0\ .$$

Near R^{SS} solutions to Eqs. (4.1) and (4.6) with the boundary conditions (2.2) may be obtained perturbatively,

$$\begin{aligned} w&=Aw_1+A^2w_2+A^3w_3+\cdots\ ,\\ \theta&=A\theta_1+A^2\theta_2+A^3\theta_3+\cdots\ , \end{aligned} \tag{4.7}$$

and likewise for u, v, and Σ, where

$$R=R^{SS}+AR_1+A^2R_2+\cdots\ . \tag{4.8}$$

Here A denotes the pattern amplitude. At leading order in A, Eq. (4.1) has solutions in the form of rolls, squares, and hexagons:

(R),

$$w_1^R=\cos(k_c x_1)\sin(\pi y)\ , \tag{4.9a}$$

(S),

$$w_1^S=[\cos(k_c x_1)+\cos(k_c x_2)]\sin(\pi y)\ . \tag{4.9b}$$

(H) ,

$$w_1^H=\{\cos(k_c x_1)+\cos[k_c(\sqrt{3}x_2-x_1)/2] + \cos[k_c(\sqrt{3}x_2+x_1)/2]\}\sin(\pi y) . \quad (4.9c)$$

In the case of hexagons, Eqs. (4.6) are solved at linear order by

$$\theta_1^H=\frac{2w_1^H}{3\pi^2},\quad \Sigma_1^H=\frac{2(1+\tau)w_1^H}{3\pi^2\tau} ,$$
$$u_1^H=\frac{2}{\pi^2}\frac{\partial^2 w_1^H}{\partial x_1\partial y},\quad v_1^H=\frac{2}{\pi^2}\frac{\partial^2 w_1^H}{\partial x_2\partial y} , \quad (4.10)$$

with similar expressions holding for rolls and squares.

At second order, Eq. (4.1) has the form

$$L_0 w_2=R_1 L_1 w_1+N_1(\mathbf{u}_1,\mathbf{u}_1) + R^{SS}[N_2(\mathbf{u}_1,\theta_1)+N_3(\mathbf{u}_1,\Sigma_1)] . \quad (4.11)$$

This is an equation for w_2, with R_1 determined by the condition that the solution be spatially periodic. Therefore, all terms on the right-hand side of Eq. (4.11) lying in the kernel of the operator L_0 must vanish. For each of the solutions considered none of the nonlinear terms in (4.11) lie in the kernel of L_0. It follows that

$$R_1^R=0,\quad R_1^S=0,\quad R_1^H=0 . \quad (4.12)$$

This condition is a consequence of symmetry as discussed in Sec. III. Equation (4.11) has solutions:

(R) ,

$$w_2^R=0 , \quad (4.13a)$$

(S) ,

$$w_2^S=\alpha f(x_1,x_2)\sin(2\pi y) \quad (4.13b)$$

(H) ,

$$w_2^H=[\beta_1 g_1(x_1,x_2)+\beta_2 g_2(x_1,x_2)]\sin(2\pi y) , \quad (4.13c)$$

where

$$f(x_1,x_2)=\cos(k_c x_1+k_c x_2)+\cos(k_c x_1-k_c x_2) ,$$
$$g_1(x_1,x_2)=\cos(k_c x_1)+\cos[k_c(\sqrt{3}x_2-x_1)/2] + \cos[k_c(\sqrt{3}x_2+x_1)/2] , \quad (4.14)$$
$$g_2(x_1,x_2)=\cos[k_c(\sqrt{3}x_2+3x_1)/2] + \cos[k_c(\sqrt{3}x_2-3x_1)/2]+\cos(\sqrt{3}k_c x_2) ,$$

and

$$\alpha=-\frac{6}{473\pi}\left[\frac{5}{\sigma}+\frac{3}{2}\left[1+\frac{S}{\tau^2}r^{SS}\right]\right] ,$$
$$\beta_1=-\frac{1}{26\pi}\left[\frac{3}{2\sigma}+\frac{1}{2}\left[1+\frac{S}{\tau^2}r^{SS}\right]\right] , \quad (4.15)$$
$$\beta_2=-\frac{9}{1250\pi}\left[\frac{11}{2\sigma}+\frac{3}{2}\left[1+\frac{S}{\tau^2}r^{SS}\right]\right] ,$$

where

$$r^{SS}\equiv\left[\frac{4}{27\pi^4}\right]R^{SS}=\frac{\tau}{\tau+S(\tau+1)} . \quad (4.16)$$

For rolls, the corresponding solutions to Eq. (4.6) are

$$u_2^R=v_2^R=0 ,$$
$$\theta_2^R=-\frac{1}{12\pi^3}\sin(2\pi y) , \quad (4.17)$$
$$\Sigma_2^R=-\frac{(\tau^2+\tau+1)}{12\pi^3\tau^2}\sin(2\pi y) ,$$

while for squares,

$$u_2^S=\frac{1}{\pi^2}\frac{\partial^2 w_2^S}{\partial y\,\partial x_1} ,$$
$$v_2^S=\frac{1}{\pi^2}\frac{\partial^2 w_2^S}{\partial y\,\partial x_2} , \quad (4.18)$$
$$\theta_2^S=\frac{1}{30\pi^3}[-5+(6\pi\alpha-2)f(x_1,x_2)]\sin(2\pi y) ,$$
$$\Sigma_2^S=\frac{(\tau^2+\tau+1)}{30\pi^3\tau^2}\left[-5+\left[\frac{6\pi\tau(\tau+1)\alpha}{\tau^2+\tau+1}-2\right]f(x_1,x_2)\right] \times\sin(2\pi y) .$$

Finally, the solutions in the case of hexagons are

$$u_2^H=\left[\frac{4}{\pi}\beta_1\frac{\partial g_1}{\partial x_1}+\frac{4}{3\pi}\beta_2\frac{\partial g_2}{\partial x_1}\right]\cos(2\pi y) ,$$
$$v_2^H=\left[\frac{4}{\pi}\beta_1\frac{\partial g_1}{\partial x_2}+\frac{4}{3\pi}\beta_2\frac{\partial g_2}{\partial x_2}\right]\cos(2\pi y) , \quad (4.19)$$
$$\theta_2^H=\left[-\frac{1}{4\pi^3}+\frac{(2\pi\beta_1-1)}{9\pi^3}g_1+\frac{(6\pi\beta_2-1)}{33\pi^3}g_2\right]\sin(2\pi y) ,$$
$$\Sigma_2^H=\frac{(\tau^2+\tau+1)}{\pi^3\tau^2}\left[-\frac{1}{4}+\frac{1}{9}\left[\frac{2\pi\tau(\tau+1)\beta_1}{\tau^2+\tau+1}-1\right]g_1 + \frac{1}{33}\left[\frac{6\pi\tau(\tau+1)\beta_2}{\tau^2+\tau+1}-1\right]g_2\right]\sin(2\pi y)$$

At third order, Eq. (4.1) has the form

$$L_0 w_3=R_2 L_1 w_1+R^{SS}[N_2(\mathbf{u}_1,\theta_2)+N_2(\mathbf{u}_2,\theta_1) + N_3(\mathbf{u}_1,\Sigma_2)+N_3(\mathbf{u}_2,\Sigma_1)] + N_1(\mathbf{u}_1,\mathbf{u}_2)+N_1(\mathbf{u}_2,\mathbf{u}_1) . \quad (4.20)$$

The solvability condition determines R_2 for rolls, squares, and hexagons. We obtain

$$R_2^R=\left[\frac{27\pi^2}{48}\right]\left[\frac{\tau^3+S(\tau^3+\tau^2+\tau+1)}{\tau[\tau+S(\tau+1)]^2}\right] , \quad (4.21a)$$

$$R_2^S=\frac{12}{5}\left[R_2^R+\frac{473\pi^4}{32}\alpha^2 r^{SS}\right] , \quad (4.21b)$$

$$R_2^H=\frac{45}{11}\left[R_2^R+\left[\frac{143\pi^4}{10}\beta_1^2+\frac{125\pi^4}{18}\beta_2^2\right]r^{SS}\right] . \quad (4.21c)$$

A. Square lattice results

We are now in a position to calculate the coefficients m and ϵ_1 in the D_4-equivariant normal form (3.9). The results for R_2^R and R_2^S given by (4.21a) and (4.21b) may be substituted into Eqs. (3.15) to give

$$\epsilon_1 = -\mathrm{sgn}\left[R_2^R + \frac{1419\pi^4}{16}\alpha^2 r^{SS}\right], \tag{4.22a}$$

$$m = \epsilon_1 \left[\frac{96R_2^R + 1419\pi^4\alpha^2 r^{SS}}{16R_2^R + 1419\pi^4\alpha^2 r^{SS}}\right]. \tag{4.22b}$$

From the general analysis of Sec. III A we know that stable nontrivial solutions exist on a neighborhood of the bifurcation point only if both squares and rolls bifurcate supercritically (i.e., $R_2^R > 0$, $R_2^S > 0$). Which of these two branches is actually stable depends on the value of ϵ_1. From the condition that the steady-state bifurcation occurs before the Hopf (2.6), it follows that

$$r^{SS} > 0 . \tag{4.23}$$

Consequently, when rolls bifurcate supercritically

$$\epsilon_1 = -1, \quad m < -1 . \tag{4.24}$$

Hence squares are never stable for physical values of τ and σ.

The degeneracies (3.10) in the vector field (3.8) occur when the following conditions are met:

$$\begin{aligned} &R_2^R = 0 \quad (p_N = q) , \\ &R_2^S = 0 \quad (p_N = 0) , \\ &R_2^S = 2R_2^R \quad (q = 0) . \end{aligned} \tag{4.25}$$

The location of these degeneracies in the (τ, S) plane is shown in Fig. 3 for two different values of σ, together with the bifurcation diagrams characteristic of the various regions of the plane. The two values of Prandtl number, $\sigma = 0.6$ and $\sigma = 18$, are appropriate to convection experiments on normal ^{3}He-^{4}He mixtures[18] and to convection experiments on ethanol-water mixtures.[5,6,19]

B. Hexagonal lattice results

The results for R_2^R and R_2^H given by (4.21a) and (4.21c) may be substituted into (3.25) to determine the coefficient a in the equivariant vector field (3.21), as well as $\mathrm{sgn}[l_3(\mathbf{0})]$. We find

$$a = -\left[\frac{68R_2^R + (1287\beta_1^2 + 625\beta_2^2)\pi^4 r^{SS}}{24R_2^R + (1287\beta_1^2 + 625\beta_2^2)\pi^4 r^{SS}}\right], \tag{4.26}$$

$$\mathrm{sgn}(l_3(\mathbf{0})) = \mathrm{sgn}\left[R_2^R + (1287\beta_1^2 + 625\beta_2^2)\frac{\pi^4 r^{SS}}{24}\right] .$$

From the general analysis presented in Sec. III B we know that stable nontrivial solution branches exist on a neighborhood of the bifurcation point only when all branches are supercritical. In the case where rolls are supercritical,

$$a < -1, \quad \mathrm{sgn}(l_3(\mathbf{0})) = +1 . \tag{4.27}$$

Hence, rolls are stable when they bifurcate supercritically. The necessary conditions for stable triangles and hexagons [$a > -\frac{1}{3}$, $\mathrm{sgn}(l_3(\mathbf{0})) = -1$] cannot be satisfied.

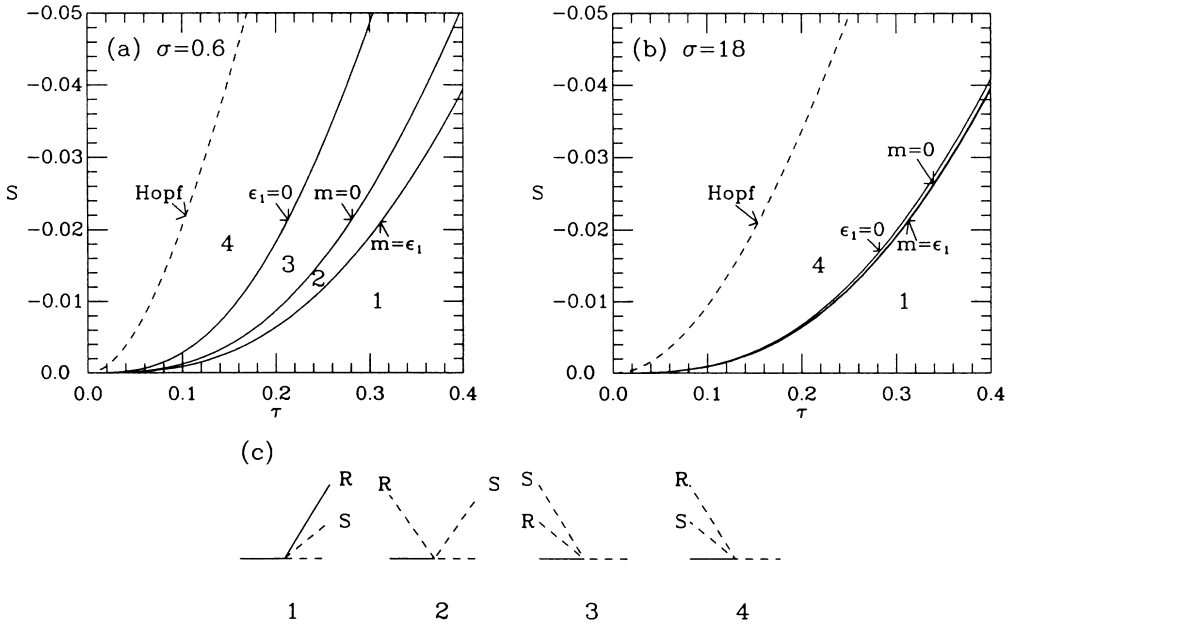

FIG. 3. Degeneracies in the D_4-equivariant normal form (3.9) are indicated by solid lines in the (τ-S) plane for (a) $\sigma = 0.6$ and (b) $\sigma = 18$. These lines separate the parameter space into four regions characterized by the bifurcation diagrams shown in (c). In (b) regions 2 and 3 have not been labeled. Above the dashed lines in (a) and (b) the initial instability is to an oscillatory state, not studied in this paper.

Degeneracies occur in (3.21) when the following conditions are met:

$$\begin{aligned} &R_2^R=0 \quad (a=-1)\,, \\ &R_2^R+R_2^H=0 \quad (a=-\tfrac{1}{2})\,, \\ &R_2^H=0 \quad (a=-\tfrac{1}{3})\,, \\ &R_2^H-3R_2^R=0 \quad [l_3(\mathbf{0})=0]\,. \end{aligned} \tag{4.28}$$

These codimension-one surfaces are shown in Fig. 4 for $\sigma=0.6$ and $\sigma=18$. They divide the (τ,S) plane into five regions, each of which is characterized by a nondegenerate bifurcation diagram as indicated.

V. DISCUSSION AND CONCLUSIONS

In this paper we have studied pattern selection in binary fluid mixtures near a bifurcation to steady convection. The problem was formulated on a doubly periodic lattice in order that rigorous results from equivariant bifurcation theory could be applied. These results apply whenever the boundary conditions do not change the assumed symmetry and specify precisely the calculations that have to be performed to solve a given pattern selection problem. Both square and hexagonal lattices were considered. In the case of the square lattice, the midplane reflection symmetry acts trivially so that the form of the amplitude equations does not depend on the symmetry of the boundary conditions; the results of Sec. III A thus apply not only to systems in which the boundary conditions at top and bottom are the same, but also to those, such as free surface problems, in which they are not. However, in the case of the hexagonal lattice, the presence of the midplane reflection symmetry does modify the normal form so that the results of Sec. III B are specific to systems in which the boundary conditions at the top and bottom are the same. In particular, with stress-free boundary conditions and fixed temperature and concentration at top and bottom, we have found that rolls are stable on both lattices whenever they bifurcate supercritically. For example, this is the case when $S>0$.

We can use our results to deduce those for a pure fluid ($S=0$) confined between stress-free boundaries held at fixed temperatures. For the square lattice we find

$$\varepsilon_1=-1, \quad m<\varepsilon_1\,, \tag{5.1}$$

while for the hexagonal lattice

$$a<-1, \quad \mathrm{sgn}(l_3(\mathbf{0}))=+1\,. \tag{5.2}$$

Note that here the rolls always bifurcate supercritically; in both cases they are stable. None of the degeneracies found in the analysis of convection in a binary fluid arise in pure fluid convection. These results are in agreement with those of Schlüter *et al.*[1] obtained by other means.

Our results may also be transformed into those for doubly diffusive convection in which the solute gradient is imposed through the boundary conditions on the concentration, instead of developing in response to an applied temperature gradient by means of the Soret effect. In this system the concentration Rayleigh number

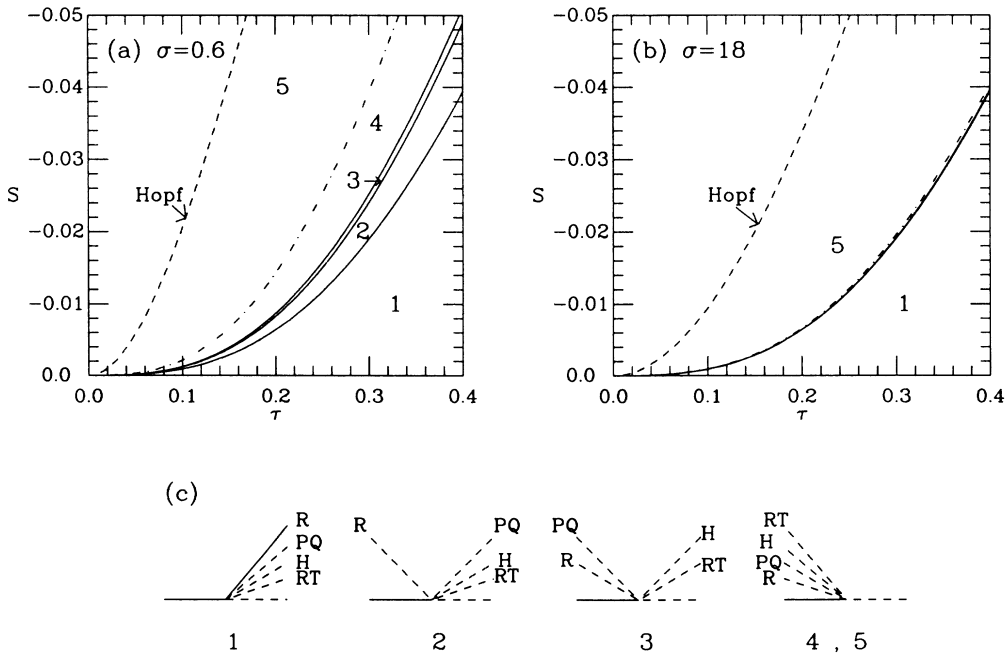

FIG. 4. Degeneracies $a=-1$, $a=-\frac{1}{2}$, $a=-\frac{1}{3}$ in the general Γ_H-equivariant vector field (3.21) are indicated by solid lines in the (τ-S) parameter space for (a) $\sigma=0.6$ and (b) $\sigma=18$. In (b) these lines are indistinguishable, and regions 2–4 have not been labeled. The coefficient a in (3.21) increases with decreasing τ and S from region 1 ($a<-1$) through region 4 ($a>-\frac{1}{3}$). The dashed-dotted line corresponds to $l_3(\mathbf{0})=0$; above it, in region 5, $l_3(\mathbf{0})<0$ and $a<-1$. The bifurcation diagrams appropriate to the various parameter regimes are shown in (c). Above the dashed lines in (a) and (b), the initial instability is a Hopf bifurcation.

$R_S \equiv -RS$ replaces the parameter S as the parameter of interest, and the term involving θ in Eq. (2.1c) is absent. Under the transformation[12]

$$R_T = R\left(1-\frac{S\tau}{1-\tau}\right), \quad R_S = \frac{-RS}{1-\tau}, \tag{5.3}$$

our results agree with those of Nagata and Thomas.[20] Applying the theory summarized in Sec. III, we conclude that rolls are stable on both the square and hexagonal lattice, whenever they bifurcate supercritically.

In this paper we have emphasized the presence of degeneracies in the bifurcation analysis. These occur along codimension-one surfaces in parameter space, and divide it into regions characterized by structurally stable bifurcation diagrams. Our interest in these degeneracies stems from the plausible hypothesis that subcritical branches turn around at large amplitude and acquire stability. Thus the transition from a supercritical bifurcation to a subcritical bifurcation (the "tricritical" point) heralds the appearance of a hysteretic transition to a stable pattern. Consider, for example, the hexagonal lattice (Fig. 4). Decreasing τ or S from a region of stable rolls one first crosses the line $a=-1$ (the tricritical point for rolls), suggesting a hysteretic bifurcation to rolls for $-1<a<-\frac{1}{2}$. The point $a=-\frac{1}{2}$ is the tricritical point for the rectangle solution (PQ), but this solution does not acquire stability when it turns around since it remains unstable to rolls. In fact, one expects a hysteretic transition to a roll pattern for all $a>-1$. Of more interest is the square lattice, where the line $m=\varepsilon_1$ is the tricritical point for rolls, and $m=0$ is the tricritical point for squares. When $\varepsilon_1=-1$, squares are unstable to rolls, whereas when $\varepsilon_1=+1$, rolls are unstable to squares. For $\varepsilon_1=-1$, $m>0$, both rolls and squares are subcritical, with squares unstable to rolls; we therefore expect the initial bifurcation to evolve to finite amplitude rolls. When $\varepsilon_1=+1$, $m>1$, the rolls are unstable to squares and we expect the initial instability to evolve to finite amplitude squares. Note that the latter situation pertains for sufficiently negative values of S.

The above suggestions can be verified by a singularity theory analysis near the codimension-two degeneracies. Such an analysis has been carried out for the square lattice[21] but not the hexagonal lattice with the extra midplane reflection symmetry. For the square lattice one picks up the conjectured saddle-node bifurcations on the (R) and (S) branches by analyzing the degeneracies $\lambda=m-\varepsilon_1=0$ and $\lambda=m=0$, respectively. Of greater interest is the degeneracy $\lambda=\varepsilon_1=0$, where there is the possibility of secondary bifurcations which produce a mixed mode branch joining the roll and square branches. For example, for $m<0$, stability may be transferred from rolls to squares via this secondary branch when $\varepsilon_1\approx 0$ is negative.[22] Two cases are possible, since the transition from stable rolls to stable squares may or may not be accompanied by hysteresis.[21] By analyzing the codimension-three degeneracy $\lambda=\varepsilon_1=m=0$, one can further show that the mixed mode branch (r_1,r_2), $r_1\neq r_2$, can undergo a tertiary Hopf bifurcation, leading to time dependence.[23] As λ is varied, the oscillation amplitude increases, and the oscillations eventually disappear in a homoclinic bifurcation.[23] The unfoldings of all four degeneracies ($m=\varepsilon_1$, $m=0$, $\varepsilon_1=0$, $m=\varepsilon_1=0$) have been analyzed and classified in considerable detail in the context of the amplitude equations for the Hopf bifurcation with O(2) symmetry[21,23] and capture the most interesting possibilities that can occur generically on the square lattice. As shown in the present paper, the codimension-two degeneracies can be obtained in steady binary-fluid convection for physical parameter values and the boundary conditions (2.2). It is possible that with other boundary conditions not only these but also the codimension-three degeneracy will occur at finite parameter values. The resulting oscillations may develop into those reported in Ref. 7 as parameters are varied away from the degeneracy. However, the no-mass-flux boundary condition must be used in order that the initial bifurcation can be to a stable square pattern.[4]

ACKNOWLEDGMENTS

The research reported here was supported by the California Space Institute (CALSPACE) and the Applied and Computational Mathematics Program of the Defense Advanced Research Projects Agency (DARPA), U. S. Department of Defense.

[1]A. Schlüter, D. Lortz, and F. Busse, J. Fluid Mech. **23**, 129 (1965).

[2]F. H. Busse, J. Fluid Mech. **30**, 625 (1967); Rep. Prog. Phys. **41**, 1929 (1978).

[3]D. S. Oliver and J. R. Booker, Geophys. Astrophys. Fluid Dyn. **27**, 73 (1983); F. H. Busse and H. Frick, J. Fluid Mech. **150**, 451 (1985).

[4]F. H. Busse and N. Riahi, J. Fluid Mech. **96**, 243 (1980); M. R. E. Proctor, *ibid.* **113**, 469 (1981); V. L. Gertsberg and G. I. Sivashinsky, Prog. Theor. Phys. **66**, 1219 (1981).

[5]R. W. Walden, P. Kolodner, A. Passner, and C. M. Surko, Phys. Rev. Lett. **55**, 496 (1985).

[6]E. Moses and V. Steinberg, Phys. Rev. Lett. **57**, 2018 (1986).

[7]P. Le Gal, A. Pocheau, and V. Croquette, Phys. Rev. Lett. **54**, 2501 (1985).

[8]M. Golubitsky and D. G. Schaeffer, *Singularities and Groups in Bifurcation Theory: Volume I*, Vol. 51 of *Springer Series in Applied Mathematical Science* (Springer, Berlin, 1985); M. Golubitsky, I. N. Stewart, and D. G. Schaeffer, *Singularities and Groups in Bifurcation Theory: Volume II*, Vol. 69 of *Springer Series in Applied Mathematical Science* (Springer, Berlin, 1988).

[9]E. Buzano and M. Golubitsky, Philos. Trans. R. Soc. London, Ser. A **308**, 617 (1983).

[10]M. Golubitsky, J. W. Swift, and E. Knobloch, Physica D **10**, 249 (1984).

[11]D. T. J. Hurle and E. Jakeman, J. Fluid Mech. **47**, 667 (1971).
[12]E. Knobloch, Phys. Fluids **23**, 1918 (1980).
[13]S. J. Linz and M. Lücke, Phys. Rev. A **35**, 3997 (1987).
[14]E. Knobloch and D. R. Moore, Phys. Rev. A **37**, 860 (1988); see also B. J. A. Zielinska and H. R. Brand, Phys. Rev. A **35**, 4349 (1987).
[15]J. Guckenheimer and P. Holmes, *Nonlinear Oscillations, Dynamical Systems and Bifurcations of Vector Fields,* Vol. 42 of *Springer Series in Applied Mathematical Science* (Springer, Berlin, 1983).
[16]M. Golubitsky and I. Stewart, Arch. Rat. Mech. Anal. **87**, 107 (1985).
[17]J. W. Swift, Ph.D. thesis, University of California, Berkeley, 1984.
[18]G. Ahlers and I. Rehberg, Phys. Rev. Lett. **56**, 1373 (1986).
[19]R. Heinrichs, G. Ahlers and D. S. Cannell, Phys. Rev. A **35**, 2761 (1987).
[20]W. Nagata and J. W. Thomas, SIAM J. Math. Anal. **17**, 91 (1986).
[21]M. Golubitsky and M. Roberts, J. Diff. Eq. **69**, 216 (1987); J. D. Crawford and E. Knobloch, Physica D (to be published).
[22]To analyze this degeneracy ε_1 is treated as an unfolding parameter and is not scaled to ± 1.
[23]E. Knobloch, Contemp. Math. **56**, 193 (1986).